

Photoemission, autoionization, and x-ray-absorption spectroscopy of ultrathin-film C₆₀ on Au(110)

A. J. Maxwell, P. A. Brühwiler, A. Nilsson, and N. Mårtensson
Department of Physics, Uppsala University, Box 530, S-751 21 Uppsala, Sweden

P. Rudolf

Laboratorio Technologie, Avanzate Superfici Catalisi—Istituto Nazionale de Fisica della Materia, Padriciano 99, I-34012, Trieste, Italy

(Received 14 June 1993)

The occupied and unoccupied electronic states of C₆₀ have been studied for single monolayer and multilayer coverages on Au(110). Only the electronic structure of the first layer, which is chemisorbed, is changed by the interaction with the substrate, due to hybridization with the possibility of charge transfer. There is no measurable bonding interaction with the second layer, which has essentially the same electronic structure as the thick film. The unoccupied electronic states below the ionization level are shown to be largely localized around the C₆₀ molecule. The energy levels of the molecules not in direct contact with the substrate are referenced to the vacuum level.

I. INTRODUCTION

A great deal of work has been carried out on the C₆₀ molecule since the discovery of a method for producing and purifying it in macroscopic quantities.¹ There is enormous interest in the electronic structure of the molecule, especially because of the superconductivity observed at unexpectedly high temperatures in alkali-metal doped fullerenes. The crystal structure of solid C₆₀ at room temperature is fcc, and the molecules rotate rapidly.² The intermolecular bonding is generally thought to be van der Waals,³ although significant intermolecular hopping contributions have been indicated by theory.⁴

Many electron and soft x-ray spectroscopic studies have been carried out on a pure C₆₀ solid.^{5–8} Extremely sharp features are seen in the occupied and unoccupied valence levels, resembling spectra for small molecules rather than those for other pure forms of solid carbon. Similar studies have been carried out on alkali-metal doped compounds.^{9,10} In particular the electronic structures of K₃C₆₀ and K₆C₆₀ have been understood in terms of complete charge transfer of the K 4s electrons to the LUMO (lowest unoccupied molecular orbital) of C₆₀.¹¹ In the case of K₃C₆₀ the LUMO becomes a partly filled band at the Fermi level, and the compound is believed to be a conductor at room temperature, though there have been suggestions that it is a doped Mott-Hubbard insulator.¹² For K₆C₆₀ the LUMO is fully occupied with six electrons, and there is an intramolecular band gap around the Fermi level.

It would be interesting to compare the bonding in these compounds with that of C₆₀ on a metal surface. Indeed STM (scanning tunneling microscopy) studies have been carried out using several different substrates,^{13–16} and in one case a strong bond has been surmised between C₆₀ and Au(111). A study combining NEXAFS (near-edge x-ray-absorption fine structure),¹⁷ LEED (low-energy electron diffraction), and photoemission¹⁸ indicated that a charge-transfer-type interaction occurs for a monolayer

of C₆₀ adsorbed on Cu(100), with charge from the substrate moving into the LUMO. There it was concluded that shifts observed in the C 1s binding energy are due to this charge transfer. Another study using photoemission and inverse photoemission¹⁹ interpreted changes in the C 1s line shape and shake-up structures as evidence of chemisorption on several substrates. This study concluded that the energy levels for a thick film are aligned on the substrate Fermi level. Raman scattering and photoemission of C₆₀ on polycrystalline noble-metal surfaces²⁰ provided further evidence of charge transfer to the LUMO, while coverage-dependent binding energy shifts in the C 1s line were also observed. The charge-transfer model is supported by model calculations, which suggest that the amount of charge transferred is dependent on the choice of substrate.²¹

We have studied the electronic structure of the first layer of C₆₀ on Au(110) using photoemission, autoionization, and NEXAFS. We have also investigated the evolution of the occupied and unoccupied electronic states with film thickness. The first layer is chemisorbed, and its electronic structure changes due to interaction with the substrate. In films thicker than 1 ML (monolayer) the electronic structure of C₆₀ molecules not in direct contact with the substrate is essentially independent of coverage. However, the binding energies of all core and valence levels shift with film thickness in a manner consistent with van der Waals bonding, such that the energy levels are properly referenced to the vacuum level.

II. EXPERIMENTAL DETAILS

The majority of spectra were taken at Beamline 22 of MAX-lab in Lund, which consists of a modified SX700 monochromator as well as a high efficiency electron spectrometer.²² Calibration of absorption spectra was carried out by measuring the photon energy, using the Au 4f_{7/2} core line or C₆₀ HOMO (highest occupied molecular orbital) excited by first- and second-order light. Binding en-

ergies in photoemission were calibrated by measuring the Fermi level, or Au $4f_{7/2}$ core line, whose position relative to the Fermi level did not change for coverages greater than 1 ML. Shake-up spectra were taken on a high-resolution electron spectrometer at Uppsala University using monochromatized AlK α x rays. Pure C₆₀ was purchased from a commercial source, the purity of which we checked by mass spectrometry. Films were evaporated from a degassed tantalum crucible onto a clean single-crystal Au(110) substrate. Pressure during evaporations was 5×10^{-10} torr. Pressure during measurements was 5×10^{-11} torr. Reproducibility of the C₆₀ evaporations was guaranteed by monitoring the temperature of the source.

The C₆₀ coverage for a complete monolayer was determined from the appearance of a second component in the C 1s spectra due to multilayer growth, an observation supported by other photoemission studies.¹⁸ Single monolayers could also be prepared by heating a thick film to approximately 450 °C, after which a single C 1s line was observed at 284.4-eV binding energy. Subsequent monolayers were deposited from an estimate of the time for deposition of 1 ML. The quality of the films is best judged by the C 1s linewidths, which indicate that there were no significant distributions of film thickness for a given nominal coverage.

III. RESULTS

A. NEXAFS

NEXAFS allows one to study the local unoccupied states of a system by measuring the absorption close to a core-level ionization threshold. In the present case we excite the C 1s electron to the unoccupied C₆₀ π manifold, i.e., LUMO, LUMO+1, etc., where we use the description of Martins, Troullier, and Weaver.²³ However, it is important to note that in the present case the excited electron populates molecular orbitals whose degeneracy has been broken by the symmetry-reducing effect of the core hole. The molecular orbitals of the excited system can be modeled using the $Z+1$ or equivalent core approximation, in which the core hole is simulated by the addition of unit nuclear charge at the excited atomic site. This approximation has been successful in the analysis of experimental results from solid-state and molecular systems.²⁴ The strongest peaks in the spectrum generally correspond to excitations to energy levels localized by the core hole, similar to excitons in large systems.¹⁷

In Fig. 1(a) we compare the NEXAFS spectra for 1, 2, and 3 ML, and a thick film of C₆₀ on Au(110). The raw data have been divided by a spectrum taken for clean Au(110), proportional to the monochromator throughput function over this energy range. Normalization was carried out by comparison of the σ^* features at 290–295 eV. The thick-film spectrum is similar to those reported in earlier studies,^{6,9} to our knowledge this is the first NEXAFS spectrum published for a single monolayer.

The overlayer structure and alignment of the spectra is constant for the series. However, the 1-ML spectrum is greatly broadened. Features characteristic of the thick

film return strongly already in the 2-ML spectrum; this can be seen particularly well in the difference spectrum shown in Fig. 1(b), where a weighted 1-ML spectrum (50% of total intensity) has been subtracted from the 2-ML spectrum. The C 1s binding energy for each film is indicated in the figure, and its location is discussed below.

In Fig. 1(c) we present a comparison between the C 1s NEXAFS and photoemission for 1 ML. It is clear that the center of the C 1s photoemission line coincides with the center of the C 1s–LUMO absorption feature in the NEXAFS spectrum. There is also a similarity in the line shape, with both photoemission and NEXAFS features showing a broadening to the low-energy side, as well as a pronounced asymmetry to the high-energy side with respect to the thick-film spectra. In particular we note the virtually equal broadening.

B. Autoionization

Autoionization (also commonly referred to as resonant photoemission) spectroscopy provides information on the decay of the core excited state (i.e., the final state in NEXAFS). Auger and autoionization are very similar, in that two valence electrons take part in the deexcitation of the system. These processes are diagrammed in Fig. 2 for a free molecule. In the single-particle picture of Auger a core-ionized molecule relaxes by a process in which the core hole is filled by a valence electron, while another electron is ejected carrying away the excess energy. In autoionization the initial state is neutral. Autoionization events can be divided into two categories, “participator” and “spectator” decays, as shown in Fig. 2. In the final state of the spectator decay process the excited electron remains in a previously unoccupied orbital, while a valence electron annihilates the core hole and another is ejected; this results in a two-hole–one-particle final state. In the participator process the final state is identical to photoemission, i.e., the initially excited electron participates in the decay. For excitations near threshold, the autoionization and photoemission spectra overlap.^{25,26}

We focus here on the HOMO participator, because it is the highest-kinetic-energy part of the autoionization spectrum, and easy to identify.⁷ Figure 3 shows a comparison of autoionization spectra for 1, 2, and 3 ML and a thick film, taken at a photon energy of 284.5 eV corresponding to the first absorption feature in the NEXAFS spectrum. These spectra are normalized to the Auger-like part of the spectrum, which has its peak at approximately 20-eV binding energy.⁷ A background spectrum taken at a photon energy below the first absorption feature in the NEXAFS spectrum for each coverage, and therefore containing only direct photoemission contributions, has been subtracted from these spectra. The C 1s second-order line, which is superimposed on the spectrum at a binding energy of between -0.1 and 0.7 eV depending on coverage, has also been removed. The C 1s first-order line for each coverage was used to model the second-order line shape and shake-up intensity.

The autoionization spectrum for 1 ML shows at most only a small contribution in the energy range of the HOMO participator. Stronger participator transitions

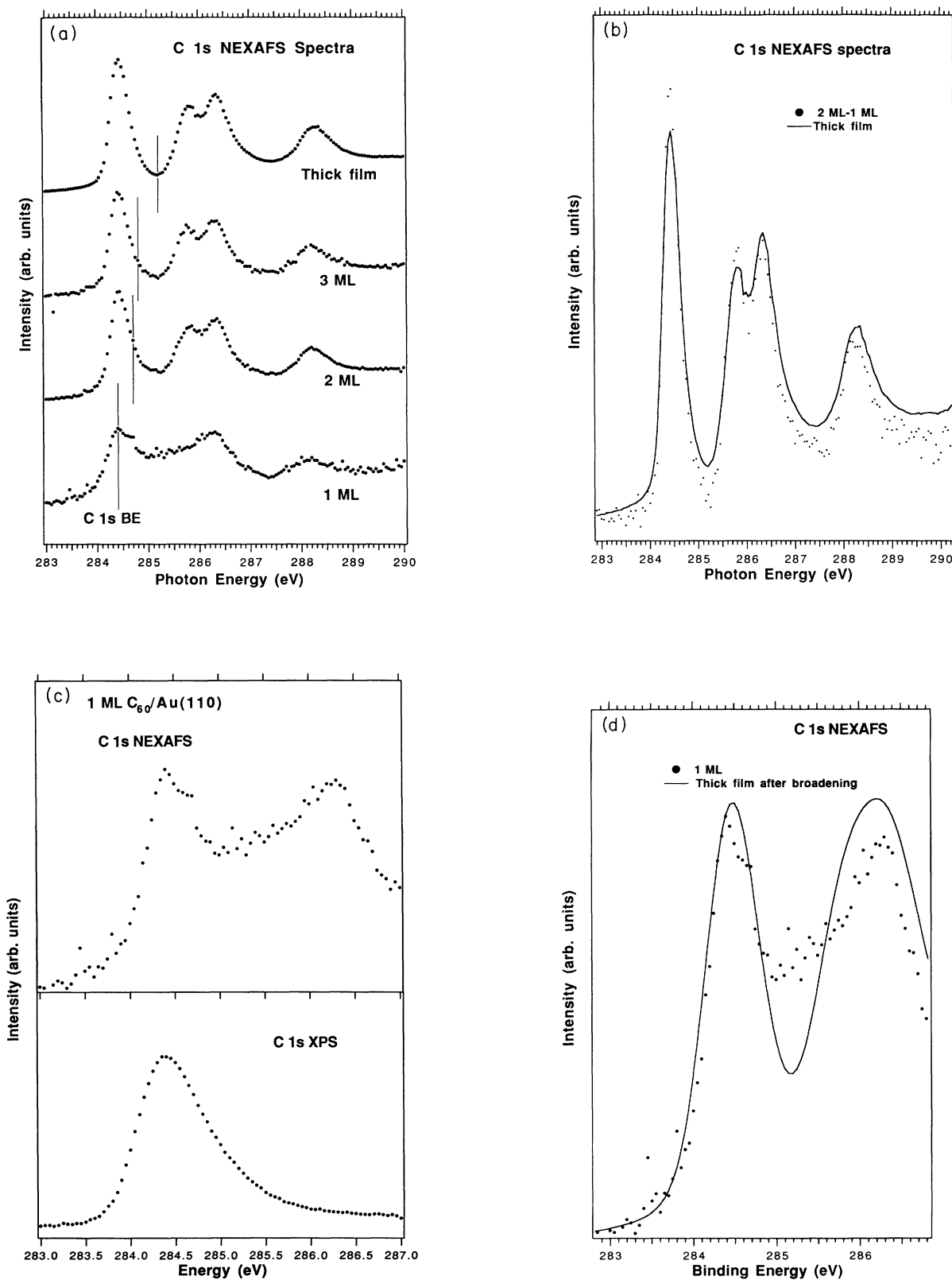


FIG. 1. $C_{60}/Au(110)$, C 1s NEXAFS spectra, (a) for the coverages indicated, where the C 1s photoemission binding energy is indicated for each coverage. (b) Comparison of the thick film spectrum and a difference spectrum calculated by subtracting the 1-ML spectrum from the 2-ML spectrum. (c) Comparison of the C 1s NEXAFS and photoemission spectra for 1 ML. (d) Comparison of the C 1s NEXAFS spectrum for 1 ML and the spectrum for a thick film, where the thick-film spectrum has been broadened by a function modeling the broadening in the C 1s photoemission line between a thick film and 1 ML.

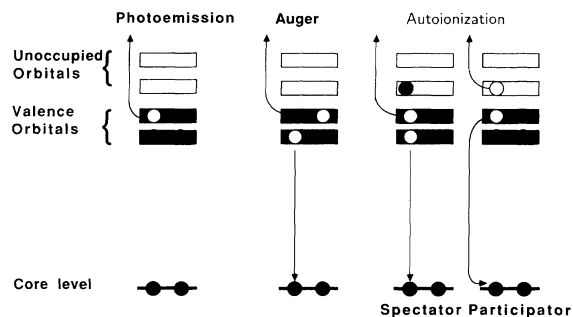


FIG. 2. Schematic diagram showing various decay processes, and comparing them to photoemission.

are observed for all higher coverages. The peak intensities for 2 and 3 ML are less than for the thick film, because the spectra are normalized to the Auger-like part of the spectrum which shows contributions from the first layer, as discussed below. The results for the thick film are identical to spectra published earlier.⁷ The binding energy of the HOMO participator is ≈ 2.0 eV for 1 ML, 2.2 eV for 2 ML, 2.3 eV for 3 ML, and 2.6 eV for a thick film.

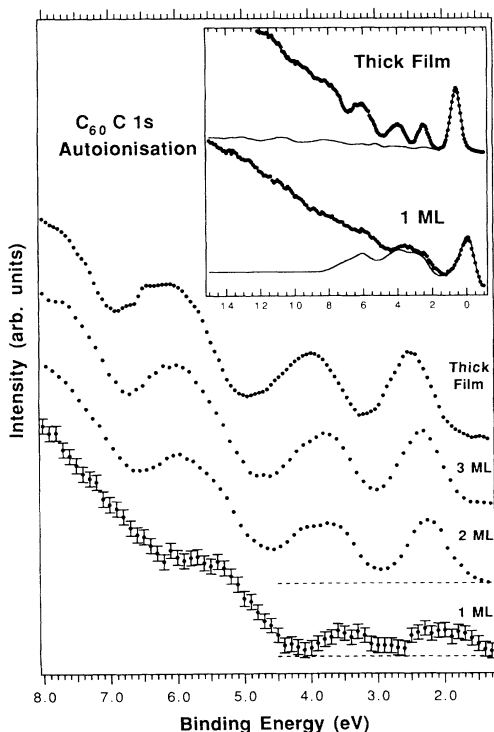


FIG. 3. C 1s autoionization spectra as a function of C_{60} layer thickness for excitation at $h\nu = 284.5$ eV, corresponding to the first absorption feature in the NEXAFS spectrum. The inset shows the original data as well as the background subtracted for the 1-ML and thick-film spectra. The background is the sum of a spectrum taken below the carbon adsorption edge, and a C 1s second-order line.

C. Valence photoemission

Figure 4(a) contains the valence photoelectron spectra of clean Au(110), 1-ML $C_{60}/Au(110)$, and a thick C_{60} film, all taken at a photon energy of 110 eV. The 1-ML spectrum shows additional structure relative to clean Au(110), which can be identified by comparison with the spectrum of the thick film, as indicated. All features shift by 0.9 eV to lower binding energy relative to those of the thick film, except the first structure below the HOMO. The HOMO is now located at a binding energy of approximately 1.7 eV, in contrast to a value of 2.6 eV for the thick-film spectrum. This is approximately the intramolecular gap energy, and led us to search for new structure near the Fermi level associated with a partly filled LUMO. However, spectra taken at widely different photon energies ($21.2 \text{ eV} < h\nu < 180 \text{ eV}$) revealed no new structure at the Fermi level. This is best seen for excitation at 21.2 eV, Fig. 4(b).

D. Core levels and shake-up

The Au $4f_{7/2}$ line before and after deposition of 1 ML C_{60} is shown in Fig. 5. Two components are observed for clean Au(110), assigned to the surface and bulk. Upon deposition of 1-ML C_{60} only one component is observed, at the same binding energy as the bulk component for clean Au(110), and this profile remains for higher coverages. There is an asymmetry to lower binding energy, which we associate with a distribution of Au sites.

In Fig. 6(a) we present the C 1s core line for C_{60} as a function of film thickness. One can see that there are great changes in the line shape and position: for a thick film the line is symmetric, lying at 285.2-eV binding energy; at 3 ML the binding energy is 284.8 eV, with a slight asymmetry to the low-binding-energy side; for 2 ML the line clearly has two components, with the main line at 284.7 eV and another peak at lower binding energy; for 1 ML the position of the peak is 284.4 eV, and the line shape shows broadening relative to all other coverages on the low-binding-energy side, as well as a pronounced asymmetry to the high-binding-energy side. The width of the C 1s line is constant for 2 and 3 ML and a thick film, and is given by a full width at half maximum equal to 0.45 eV. The C 1s shake-up spectra for 1 and 2 ML and a thick film are shown in Fig. 7. In the 1-ML spectrum the features of the thick film are apparent as broadened structures, which become sharper in the 2-ML spectrum.

IV. DISCUSSION

A. Electronic structure of the first ML

1. Formation of a chemisorption bond

In the following discussion we will present various arguments from results of the spectroscopic measurements that a true chemical bond is formed between a C_{60} monolayer and Au(110). We begin with the Au(110) $4f_{7/2}$ spectrum, shown in Fig. 5. The change in line shape of this level clearly involves the modification of the clean surface component, a pattern associated with chemisorption in previous studies of smaller adsorbates.²⁷ We as-

cribe the remaining asymmetry in the line to inequivalent Au atomic sites, consistent with the reported structure.¹⁶

It can be seen from Fig. 1(c) that the C 1s binding energy measured for 1 ML is 284.4 eV, equal to the photon energy of the NEXAFS absorption edge. It has been not-

ed previously that in the case of a metallicly screened core hole, in which the screening electron comes from the Fermi level, the core-ionized final state corresponds to the lowest x-ray-absorption final state.²⁸ The coincidence of the absorption edge and core-level binding energy can

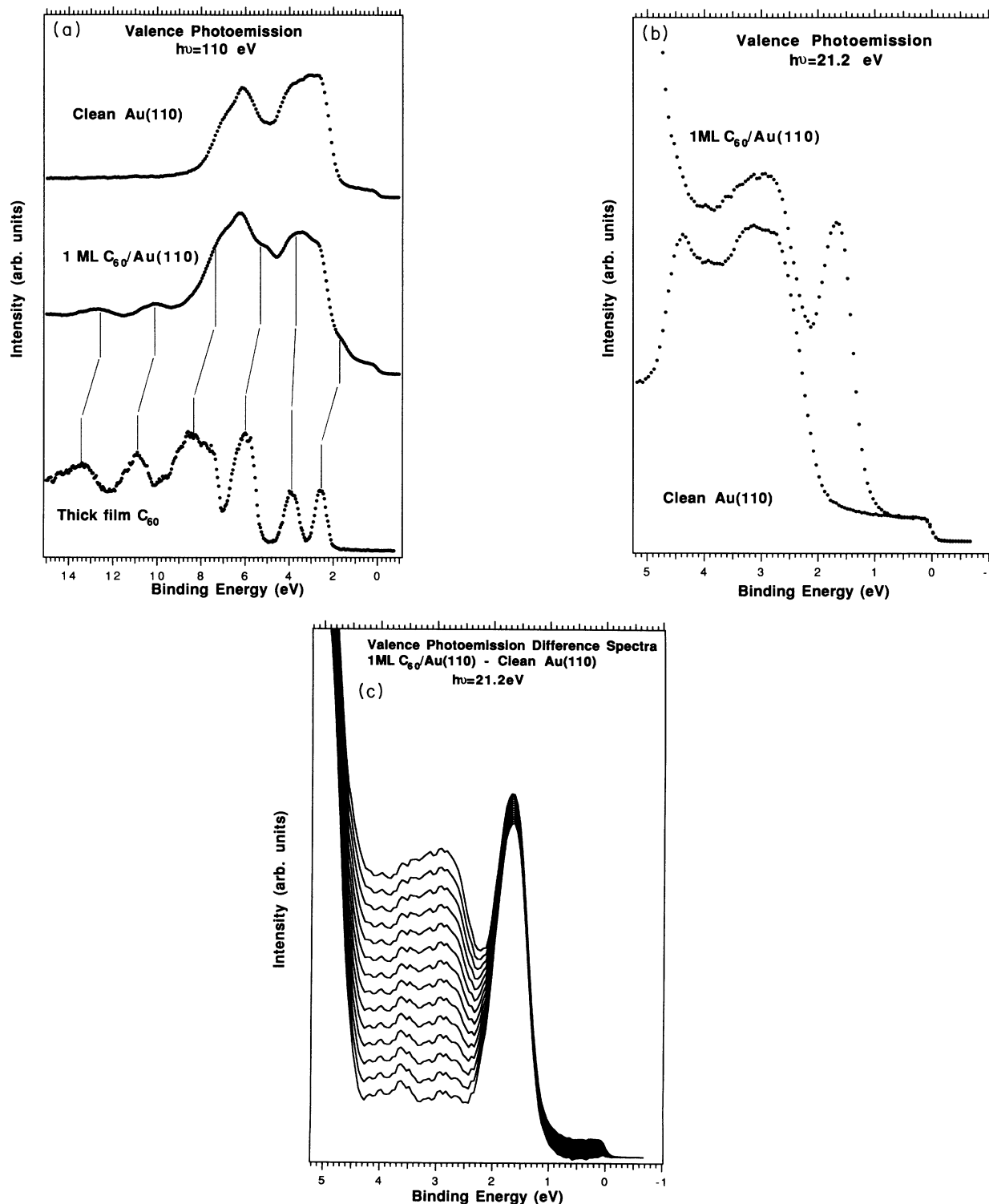


FIG. 4. Valence photoemission spectra (a) for clean Au(110), 1-ML C₆₀/Au(110), and a thick film of C₆₀, $h\nu = 110$ eV; (b) for clean Au(110) compared to 1-ML C₆₀/Au(110), $h\nu = 21.2$ eV (He I); and (c) for 1-ML C₆₀/Au(110), in which different background intensities have been subtracted to model the emission from the substrate.

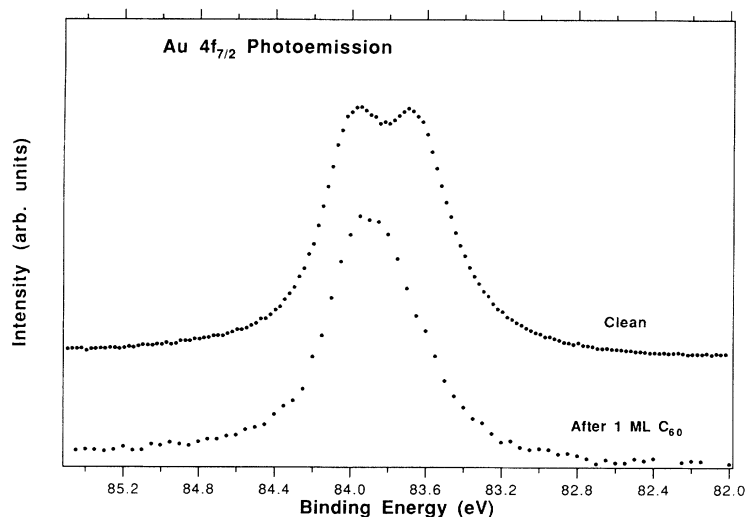


FIG. 5. Au $4f_{7/2}$ photoemission spectra, before and after deposition of 1-ML C_{60} .

therefore be explained in terms of metallic screening, providing strong evidence for a chemisorption bond in the final state through which screening charge can be redistributed between the molecule and the surface upon the creation of a core hole.

Further support for the chemisorption model is obtained by studying the C $1s$ line shape of 1-ML C_{60} , shown in Fig. 6(b). The asymmetry toward higher binding energies in the 1-ML spectrum is due to an unknown combination of two factors: the creation of electron-hole pairs in the partly filled band formed at the interface between the chemisorbed monolayer and the substrate, and site variations within the C_{60} molecule. Electron-hole pairs are certainly excited, because the LUMO is located at the Fermi level in the core-excited state, as described above. It is also clear from STM studies that great variations in atomic site exist,³⁰ which go beyond those already expected for adsorbed C_{60} due to the reconstruction induced by the adlayer. In principle, there could be an increased probability for excitation of low-energy molecular vibrations upon adsorption, as has been observed in other studies of adsorbates.³¹

The broadening observed in the 1-ML NEXAFS spectrum compared to the thick film, seen in Fig. 1(a), could be due to several factors: inequivalent carbon sites on the molecule, vibrational broadening, or hybridization in the core-excited final state.^{29,32} The first two mechanisms will also cause broadening in the C $1s$ photoemission line, discussed above. In Fig. 1(d) we present a comparison between the 1-ML spectrum, and the thick-film spectrum broadened by a function which models the increase in linewidth of the C $1s$ XPS line between the thick-film and 1-ML spectra. The NEXAFS linewidths therefore are not dominated by hybridization in the core-excited final state, and NEXAFS features can still be seen right up to the ionization threshold. However, there is an increase in intensity around 285.4 eV, and a decrease around 285.8 eV, the latter being the position of the second feature in the unbroadened thick-film spectrum. This is clear evidence of hybridization between the unoccupied valence levels of C_{60} and the substrate, and can be understood in

terms of the thick-film NEXAFS feature at 285.8 eV shifting to lower photon energy. This is consistent with our previous studies, which suggest that this level has the largest spatial extent of the first three unoccupied orbitals,^{33,34} and is therefore more likely to take part in bonding with the substrate.³⁵

From Fig. 3 one can see that the intensity due to participator autoionization decreases significantly between a thick film and single monolayer. This is due to the transfer of the excited electron from the chemisorbed molecule to the substrate Fermi level in the time scale of the deexcitation process, so that only Auger decay is possible. This intensity loss provides further direct evidence that a hybridized level is formed in the final state, i.e., between the core-hole-perturbed $5t_{1u}$ orbital ($67a'^*$; see Ref. 37) and the sp band of the Au(110) surface, with a bonding interaction of the order of several times the C $1s$ lifetime of 0.1 eV. This can be understood from our other work.³³ The autoionization spectrum for 1 ML appears to show a little intensity in the HOMO participator region, although normalization here is difficult due to the strength of the Au d bands in the direct photoemission background. A complete loss of intensity would be expected for a strongly chemisorbed species, assuming the core-hole-modified π^* orbital being probed had weight in the whole molecule.

The energy shift of all the features in the 1-ML valence spectrum of 0.9 eV relative to a thick film [see Fig. 4(a)] is consistent with the pinning of the LUMO at the Fermi level, although a crude model based on image charge screening is not inconsistent with the results (see Sec. IV C) and explains the trends in the shifts between 2 ML and a thick film. The feature directly to higher binding energy from the HOMO appears to be strongly affected by the bonding interaction; this feature is also shifted relative to all the other levels, and there is an indication of splitting in the difference spectra, Fig. 4(c). Theory indicates that this band is derived from two molecular orbitals, the $7h_g$ and $5g_g$, where one component of the symmetry-split $7h_g$ orbital is predicted to have a large dispersion in the solid,¹¹ suggesting that it may also be

more likely to take part in the bonding of the C_{60} molecule to the surface. Otherwise, the molecular electronic structure is well preserved. It is interesting to compare the results for C_{60} on Au(110) to results obtained for benzene, which has been the subject of a great deal of discussion in the past. Benzene is chemisorbed on various

transition-metal and noble-metal surfaces through hybridization of its π orbitals with the d bands of the substrates.³⁶ Changes in the binding energy of valence electrons in a C_{60} monolayer chemisorbed on Au, compared to a thick film, are similar to changes observed in the valence band of benzene on transition-metal surfaces. The $1e_{1g}$ and $1a_{2u}$ π levels in a benzene monolayer are shifted to higher binding energy, while all other structures shift approximately 0.8 eV to lower binding energy. The fact that the HOMO-derived level of C_{60} , which is also believed to have nearly pure π character,²³ follows the shift in the mainly σ -derived levels, and is apparently unperturbed by the substrate, is probably related to its binding energy falling below that of the Au d bands which have their onset at approximately 2.5 eV. The importance of the d bands is further supported by the coincidence of the d -band edge and the perturbed C_{60} π orbitals.

Further evidence for hybridization in the core-hole final state is provided by the C 1s shake-up spectrum shown in Fig. 7. The broadening of the shake-up features relative to the thick-film spectrum can be understood³⁷ in terms of hybridization between the occupied and unoccupied molecular orbitals of C_{60} and the substrate conduction band.

The coincidence of the C 1s binding energy and NEXAFS threshold, C 1s photoemission and shake-up spectra, as well as the decrease in participator autoionization, all imply overlap between the LUMO and the substrate Fermi level in the final state. Changes in the NEXAFS spectrum show hybridization between the substrate and NEXAFS features at 285.8 eV. However, the bonding interaction of the unoccupied valence levels with the sub-

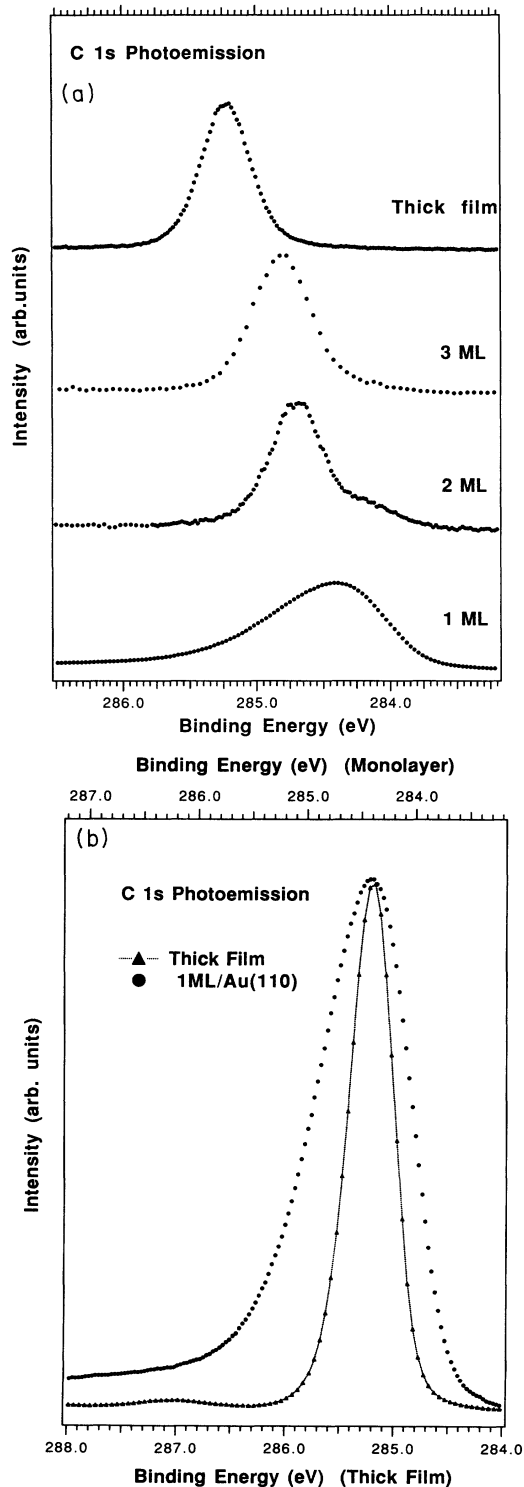


FIG. 6. C_{60} C 1s photoemission spectra, (a) for the coverages indicated on Au(110), and (b) for 1 ML and a thick film on Au(110).

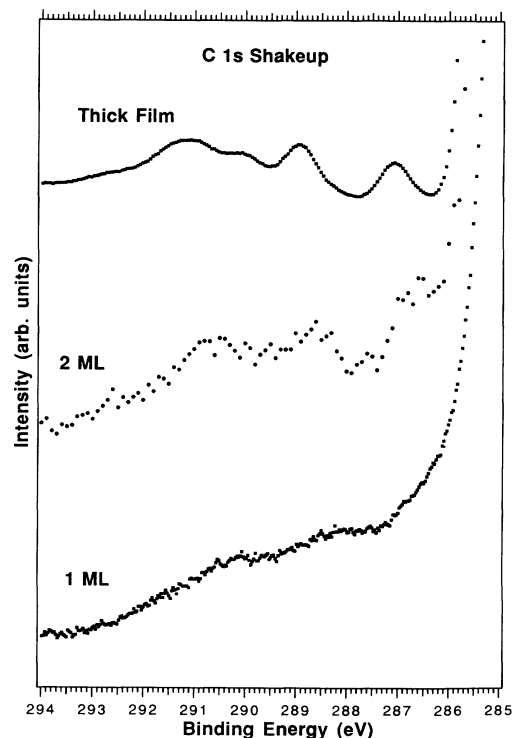


FIG. 7. C 1s shakeup spectra for coverages of 1 and 2 ML, and a thick film of $C_{60}/Au(110)$.

strate is not sufficient to dominate the NEXAFS linewidth. Changes observed in the C_{60} valence photoemission spectrum give direct evidence of hybridization between the Au d bands and C_{60} π orbitals in the ground state. The loss of the surface component from the Au(110) $4f_{7/2}$ photoemission line is also strong evidence for chemisorption in the ground state.

2. Charge transfer between the substrate and chemisorbed C_{60} monolayer

Previous reports have shown evidence of charge transfer from the conduction band of noble-metal substrates to the C_{60} LUMO,^{18,20,30} implying that the bond between C_{60} and the substrate is ionic. A charge-transfer model is at first glance unreasonable since C_{60} has an electron affinity of 2.7 eV,³⁸ and the work function of gold is 5.37 eV.³⁹ However, one must consider the self-consistent final state, taking into account charge overlap and molecular distortion. If we start with the general case of a spherical dielectric shell on a metal surface, addition of a unit electrical charge to the shell will release, in addition to the electron affinity of the isolated shell, the image potential energy given by $V = q^2/2R$. The energy gain is approximately 2 eV for this case, and should be added to the electron affinity to make a total of 4.7 eV. The molecule may distort somewhat to enhance this effect, and if the image plane were to be located inside the C_{60} molecule an even greater net electron affinity could be attained. It is therefore possible for charge to be transferred from Au(110) to the LUMO of C_{60} . However, photoemission difference spectra shown in Fig. 4(c), between 1 ML on Au(110) and the clean surface, show that we cannot identify a new feature at the Fermi level in the valence photoemission spectrum for 1-ML $C_{60}/Au(110)$, as suggested for thin C_{60} films on polycrystalline Ag and Cu.²⁰ Different substrate contributions were subtracted for comparison. A quantitative analysis is precluded due to the strong Au d bands in this region, and the possible changes in the Au conduction band at the surface due to C_{60} adsorption. The difference spectra do indicate unambiguously that any states corresponding to partial filling or hybridization of the LUMO are very broad.

B. Electronic structure of the second and subsequent layers

Changes in electronic structure for coverages greater than 1 ML are important, since they reflect the evolution of the molecular bonding to the substrate with coverage, and will turn out to provide insight into the bonding of solid C_{60} . It has been claimed that the energy levels are influenced by the substrate even in a thick film,¹⁹ implying significant electron transport among neighboring molecules. On the other hand, correlation and vibronic effects would be expected to greatly diminish or eliminate such transport, rendering C_{60} a more traditional molecular solid in this respect.

We note that in the NEXAFS spectrum for 2 ML [see Fig. 1(a)], the features of the thick-film spectrum immediately return. Indeed, if the spectrum for 1 ML is subtracted from the spectrum for 2 ML, as shown in Fig.

1(b), the result is sharp unbroadened features, similar to spectra for individual C_{60} molecules isolated in a Xe matrix.³³ The thick-film features also return in a valence photoemission difference spectrum between 1 and 2 ML. The narrowing of the line profile between 1 and 2 ML C 1s photoemission lines indicates that surface effects are not observed in the second layer. Features of the thick-film spectrum are also seen to return in the 2-ML C 1s shake-up spectrum shown in Fig. 7, in line with the NEXAFS and valence photoemission results. The second-layer spectra are strong evidence that the chemisorption bond is restricted to the first layer.

Autoionization results, shown in Fig. 3, show that the amount of participator autoionization in the second layer is approximately equal to that observed at the surface of a thick film of C_{60} . The steady increase in intensity between the HOMO participator for 2 and 3 ML and a thick film (see Fig. 3) is due to the fact that the spectra have been normalized by making the total Auger intensity equal; the 2- and 3-ML spectra show Auger contributions from the first layer. This interpretation is supported by our measurement of the electron mean free path, carried out by measuring the contributions to the C 1s line shape due to the first and subsequent layers for different thicknesses. Thus the autoionization data show that the second layer has very little hybridization with the first layer. There is no charge transfer to the second layer, as this would require a partly filled band via which the excited electron could tunnel away.

C. Relaxation effects

The shift in C 1s binding energy between 1, 2, and 3 ML and the thick film is close to the shift in the binding energy of the C_{60} valence levels discussed earlier, as shown in Table I. The chemisorption of the first layer accounts for the relatively low binding energy of the C 1s and HOMO levels for this coverage. We assign the subsequent binding-energy shifts to screening effects, because the binding-energy shifts follow a pattern found in studies of rare-gas films.⁴⁰

Charging was observed for very thick coverages, with the binding energies of the C 1s line and valence band decreasing with greater film thickness, although we have not studied this in detail. Values given here for a thick film are those measured for a "plateau" where the maximum binding energy was observed. The C 1s and HOMO binding energies have been measured by several different groups with different values obtained, e.g., for the C 1s line: 285.2 eV,⁷ 285.0 eV,¹⁰ 284.7 eV,¹⁹ and 284.5 eV.¹⁸ The binding energy of the HOMO, as well as other photoemission features, is also strongly coverage dependent and tracks the C 1s binding energy nearly perfectly as shown in Table I. Because C_{60} multilayers are

TABLE I. Binding energies of the C_{60} HOMO and C 1s line for the coverages indicated.

	1 ML	2 ML	3 ML	Thick film
HOMO	1.7 eV	2.2 eV		2.6 eV
C 1s	284.4 eV	284.7 eV	284.8 eV	285.2 eV

weakly bound, and their energy levels are aligned to the vacuum level, the importance of good coverage calibration must be stressed.

V. CONCLUSIONS

We have investigated both occupied and unoccupied electronic levels of $C_{60}/Au(110)$. In spectra taken for a carefully prepared monolayer, the C 1s binding energy coincides with the NEXAFS threshold, there is a strong decrease in participator autoionization, and a large asymmetry to higher binding energies in the C 1s photoemission line. This is all strong evidence for hybridization between the C_{60} LUMO and the occupied states around the substrate Fermi level in the core-excited final state. Changes in the NEXAFS spectrum for 1 ML compared

to a thick film show that hybridization also occurs with the unoccupied levels making up the NEXAFS feature at 285.8 eV. However, the bonding interaction is not sufficient to dominate the NEXAFS linewidth. Changes in the valence photoemission spectrum give direct evidence of hybridization between Au d bands and C_{60} π levels in the ground state. Further ground-state support for chemisorption is given by the loss in the surface component of the Au $4f_{7/2}$ photoemission line. The electronic structure of the second and third layers is very similar to that of a thick film, and the chemisorptive bond is shown to be restricted to the first layer. Binding-energy shifts of the C_{60} valence and C 1s levels as a function of coverage are consistent with a substrate image screening model, modified by increasingly important C_{60} dielectric screening as the coverage is increased.

- ¹W. Krättschmer, L. D. Lamb, K. Fostiropoulos, and D. R. Huffman, *Nature* **347**, 354 (1990).
- ²R. D. Johnson, D. S. Bethune, and C. S. Yannoni, *Acc. Chem. Res.* **25**, 169 (1992).
- ³Y. Wang, D. Tománek, and G. F. Bertsch, *Phys. Rev. B* **44**, 6562 (1991).
- ⁴O. Gunnarsson, S. Satpathy, O. Jepsen, and O. K. Andersen, *Phys. Rev. Lett.* **67**, 3002 (1991).
- ⁵J. H. Weaver, J. L. Martins, T. Komeda, Y. Chen, T. R. Ohno, G. H. Kroll, N. Troullier, R. E. Haufler, and R. E. Smalley, *Phys. Rev. Lett.* **66**, 1741 (1991).
- ⁶L. J. Terminello, D. K. Shuh, F. J. Himpsel, D. A. Lapiano-Smith, J. Stöhr, D. S. Bethune, and G. Meijer, *Chem. Phys. Lett.* **182**, 491 (1991).
- ⁷P. A. Brühwiler, A. J. Maxwell, A. Nilsson, R. L. Whetten, and N. Mårtensson, *Chem. Phys. Lett.* **193**, 311 (1992).
- ⁸P. J. Benning, D. M. Poirier, N. Troullier, J. L. Martins, J. H. Weaver, R. E. Haufler, L. P. F. Chibante, and R. E. Smalley, *Phys. Rev. B* **44**, 1962 (1991).
- ⁹C. T. Chen *et al.*, *Nature* **352**, 603 (1991).
- ¹⁰P. J. Benning, D. M. Poirier, T. R. Ohno, Y. Chen, M. B. Jost, F. Stepniak, G. H. Kroll, J. H. Weaver, J. Fure, and R. E. Smalley, *Phys. Rev. B* **45**, 6899 (1992).
- ¹¹S. Satpathy, V. P. Anropov, O. K. Andersen, O. Jepsen, O. Gunnarsson, and A. I. Liechtenstein, *Phys. Rev. B* **46**, 1773 (1992).
- ¹²R. W. Lof, M. A. van Veenendaal, B. Koopmans, H. T. Jonkman, and G. A. Sawatzky, *Phys. Rev. Lett.* **68**, 3924 (1992).
- ¹³E. Altman and R. Colton, *Surf. Sci.* **279**, 49 (1992).
- ¹⁴S. Howells, T. Chen, M. Gallagher, D. Sarid, D. Lichtenberger, L. Wright, C. Ray, D. Huffman, and L. Lamb, *Surf. Sci.* **274**, 141 (1992).
- ¹⁵Y. Z. Li, J. C. Patrin, M. Chandler, J. H. Weaver, L. P. F. Chibante, and R. E. Smalley, *Science* **252**, 547 (1991).
- ¹⁶S. Modesti, R. Schlittler, and J. Gimzewski (unpublished).
- ¹⁷J. Stöhr, *NEXAFS Spectroscopy* (Springer-Verlag, Berlin, 1992).
- ¹⁸J. E. Rowe, P. Rudolf, L. H. Tjeng, R. A. Malic, G. Meigs, C. T. Chen, J. Chen, and E. W. Plummer, *Int. J. Mod. Phys. B* **6**, 3909 (1992).
- ¹⁹T. R. Ohno, Y. Chen, S. E. Harvey, G. H. Kroll, J. H. Weaver, R. E. Haufler, and R. E. Smalley, *Phys. Rev. B* **44**, 13747 (1991).
- ²⁰S. J. Chase, W. S. Bacsa, M. G. Mitch, L. J. Pilione, and J. S. Lannin, *Phys. Rev. B* **46**, 7873 (1992).
- ²¹E. Burstein, S. C. Erwin, M. Y. Jiang, and R. P. Messmer, *Phys. Scr. T* **41**, 1 (1992).
- ²²J. N. Andersen, O. Björneholm, A. Sandell, R. Nyholm, J. Forsell, L. Thånell, A. Nilsson, and N. Mårtensson, *Synchr. Rad. News* **4**, 15 (1991).
- ²³J. L. Martins, N. Troullier, and J. H. Weaver, *Chem. Phys. Lett.* **180**, 457 (1991).
- ²⁴B. Johansson and N. Mårtensson, *Phys. Rev. B* **21**, 4427 (1980).
- ²⁵O. Björneholm, A. Sandell, A. Nilsson, N. Mårtensson, and J. N. Andersen, *Phys. Scr. T* **41**, 217 (1992).
- ²⁶W. Eberhardt, R. Dudde, M. L. M. Rocco, E. E. Koch, and S. Bernstorff, *J. Electron Spectrosc. Relat. Phenom.* **51**, 373 (1990).
- ²⁷J. N. Andersen, M. Qvarford, R. Nyholm, S. L. Sorensen, and C. Wigren, *Phys. Rev. Lett.* **67**, 2822 (1991).
- ²⁸A. Nilsson, O. Björneholm, E. O. F. Zdansky, H. Tillborg, N. Mårtensson, J. N. Andersen, and R. Nyholm, *Chem. Phys. Lett.* **197**, 12 (1992).
- ²⁹Y. Jugnet, F. J. Himpsel, P. Avouris, and E. Koch, *Phys. Rev. Lett.* **53**, 198 (1984).
- ³⁰S. Modesti, S. Cerasari, and P. Rudolf, *Phys. Rev. Lett.* **71**, 2469 (1993).
- ³¹N. Mårtensson and A. Nilsson, *J. Electron Spectrosc. Relat. Phenom.* **52**, 1 (1990).
- ³²O. Björneholm, A. Nilsson, E. O. F. Zdansky, A. Sandell, B. Hernnäs, H. Tillborg, J. N. Andersen, and N. Mårtensson, *Phys. Rev. B* **46**, 10353 (1992).
- ³³P. A. Brühwiler, A. J. Maxwell, P. Rudolf, C. D. Gutleben, B. Wästberg, and N. Mårtensson, *Phys. Rev. Lett.* **71**, 3721 (1993).
- ³⁴P. A. Brühwiler, A. J. Maxwell, and N. Mårtensson, *Int. J. Mod. Phys. B* **6**, 3923 (1992).
- ³⁵O. Björneholm, A. Nilsson, E. Zdansky, A. Sandell, H. Tillborg, J. Andersen, and N. Mårtensson, *Phys. Rev. B* **47**, 2308 (1993).
- ³⁶W. Huber, H. P. Steinrück, T. Pache, and D. Menzel, *Surf. Sci.* **217**, 103 (1989).
- ³⁷C. Enkvist, S. Lunell, B. Sjögren, S. Svensson, P. A. Brühwiler, A. Nilsson, A. J. Maxwell, and N. Mårtensson, *Phys. Rev. B* **48**, 14629 (1993).
- ³⁸R. E. Haufler, L.-S. Wang, L. P. F. Chibante, C. Jin, J. Conceicao, Y. Chai, and R. E. Smalley, *Chem. Phys. Lett.* **179**, 449 (1991).
- ³⁹B. Herbert and J. Michaelson, *Appl. Phys. A* **48**, 4729 (1977).
- ⁴⁰T. C. Chiang, G. Kaindl, and T. Mandel, *Phys. Rev. B* **33**, 33 (1986).

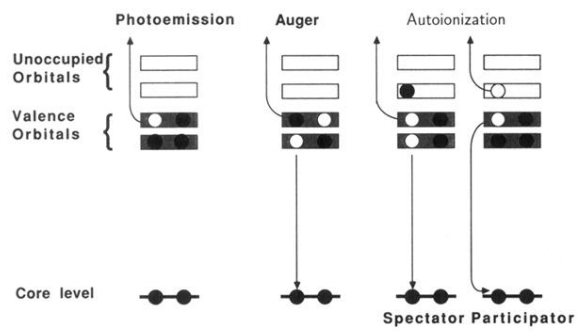


FIG. 2. Schematic diagram showing various decay processes, and comparing them to photoemission.